

## BALMER LINE PROFILES FOR INFALLING T TAURI ENVELOPES

NURIA CALVET

Centro de Investigaciones de Astronomía, Ap. Postal 264, Mérida, 5101-A, Venezuela

AND

LEE HARTMANN<sup>1</sup>

Harvard-Smithsonian Center for Astrophysics, Mail Stop 15, 60 Garden Street, Cambridge, MA 02138

Received 1991 June 3; accepted 1991 August 13

### ABSTRACT

We consider the possibility that the Balmer emission lines of T Tauri stars arise in infalling envelopes rather than winds. Line profiles for the upper Balmer lines are presented for models with cone geometry, intended to simulate the basic features of magnetospheric accretion from a circumstellar disk. An escape probability treatment is used to determine line source functions in nonspherically symmetric geometry. We find that thermalization effects can produce nearly symmetric H $\alpha$  line profiles at the same time the higher Balmer series lines exhibit inverse P Cygni profiles. The infall models produce centrally peaked emission line wings, in good agreement with observations of many T Tauri stars. Furthermore, if it is assumed that the flow follows a dipole pattern, infall models can produce narrow central absorption reversals that are slightly blueshifted when viewed from certain angles. We suggest that the Balmer emission of many T Tauri stars may be produced in an infalling envelope, with blueshifted absorption contributed by an overlying wind. Some of the observed narrow absorption components with small blueshifts may also arise in the accretion column.

*Subject headings:* accretion, accretion disks — line: profiles — stars: emission-line, Be — stars: pre-main-sequence

### 1. INTRODUCTION

The mechanism responsible for the bright ultraviolet excess continua and the strong, broad emission lines of T Tauri stars has been a puzzle for many years. The discovery of “inverse P Cygni” profiles, indicating infall of material in some T Tauri stars (Walker 1972; Appenzeller & Wolf 1977; Bertout et al. 1977; Wolf, Appenzeller, & Bertout 1977; Appenzeller, Mundt, & Wolf 1978; Edwards 1979; Mundt 1979) suggested that the energy released by mass accretion could account for the observed emission. The large velocities of the redshifted absorption imply infall from substantial distances (Walker 1972; Lamzin 1989), and the phenomenon was interpreted in terms of the end of the quasi-radial protostellar accretion phase (e.g., Ulrich 1976; Appenzeller & Wolf 1977; Bertout 1977, 1979a, b; Ulrich & Knapp 1979; Bastian 1982). The accretion interpretation eventually fell into disfavor because of the general predominance of normal P Cygni profiles in a variety of optical spectral lines (Kuhi 1964; Herbig 1977), which indicated that the material in T Tauri envelopes is predominantly flowing out. The blueshifted forbidden-line emission observed in many T Tauri stars also provides evidence for mass loss on large scales (Appenzeller, Jankovics, & Ostreicher 1984; Edwards et al. 1987).

Accretion onto T Tauri stars is now thought to proceed through circumstellar disks (Lynden-Bell & Pringle 1974; Rucinski 1985; Adams, Lada, & Shu 1987; Bertout 1987; Kenyon & Hartmann 1987; Bertout, Basri, & Bouvier 1988; Basri & Bertout 1989). The geometry of the disk model reconciles accretion and outflow, since material can fall in along the disk plane while a bipolar wind can flow outwards along the

rotational axis (Shu, Adams, & Lizano 1987). However, simple accretion disk models do not explain the existence of inverse P Cygni profiles, since the infall velocities through the disk are expected to be quite small.

The actual accretion patterns of T Tauri stars may be more complicated than implied by the standard disk model. Bertout et al. (1988) suggested that the nonaxisymmetric magnetic field of DF Tauri controls the accretion of disk material onto the star, disrupting the disk at several stellar radii above the photosphere. They proposed that a hot spot at the base of the magnetic accretion column, rotating with the star, produced the observed quasi-periodic ultraviolet excess. This idea has been developed further by Camenzind (1990) and by Königl (1991), who have postulated a disk-magnetosphere interaction similar to that of the model originally developed by Ghosh & Lamb (1979a, b) for accreting neutron stars. If the magnetospheric control of accretion extends to sufficiently large radii, then the infalling gas will develop substantial radial velocities, explaining the inverse P Cygni line profiles occasionally observed (see also Krautter, Appenzeller, & Jankovics 1990). Camenzind (1990) and Königl (1991) suggest that a large magnetosphere interacting with the circumstellar disk might play an important role in the angular momentum transfer in T Tauri systems, and help explain the observed slow rotation of pre-main-sequence stars (Vogel & Kuhi 1981; Bouvier et al. 1986; Hartmann et al. 1986).

Because inverse P Cygni profiles are not observed in most T Tauri systems, one might infer that magnetospheric effects are important only in a minority of objects. However, this conclusion could be modified by radiative transfer effects or by geometry. Ulrich (1976) and Wagenblast, Bertout, & Bastian (1982) suggested that apparently normal P Cygni profiles could be produced in infalling envelopes, but the source functions used to calculate the profiles were heuristic. Geometrical effects may also be important; for example, if accretion is confined to

<sup>1</sup> Visiting Astronomer, Kitt Peak National Observatory, operated by the National Optical Astronomy Observatory under contract to the National Science Foundation.

a thin magnetic column, redshifted absorption would not be detected unless the accretion column is aligned close to the direction of observation. An assessment of the general viability of the magnetospheric model for explaining the line profiles of T Tauri stars requires detailed radiative transfer models in non-spherically symmetric geometry.

In this paper we present calculated Balmer line profiles for infalling T Tauri envelopes. Using an approximate escape probability treatment, we find that it is possible to produce nearly symmetric emission line profiles with infall, with no apparent high-velocity redshifted absorption. The calculated line profiles exhibit reasonable agreement with observations of some T Tauri stars, observations that have proved difficult to match with simple wind models (see Hartmann et al. 1990, hereafter Paper I; Calvet, Hartmann, & Hewett 1991, hereafter Paper II). We suggest that infall may be more common in T Tauri envelopes than previously recognized.

## 2. CALCULATIONS

We adopt a coordinate system in which  $z$  is the polar axis of symmetry,  $r$  is the radial distance from the center of the star, and  $\theta$  is the angle measured from the  $z$ -axis. For most of the models discussed in this paper, we assume that material falls radially onto the star in two restricted latitude bands or "cones" in opposing hemispheres (see Fig. 1). This cone of infalling material is intended to crudely represent accretion restricted by a dipole stellar magnetic field aligned with the polar axis (e.g., Königl 1991) with a minimum of parameters. We assume that the "far-side" cone is only occulted by the star because the magnetosphere holds the disk off from the photosphere. The flow is further assumed to be steady and axisymmetric. The density is assumed to be constant on surfaces of

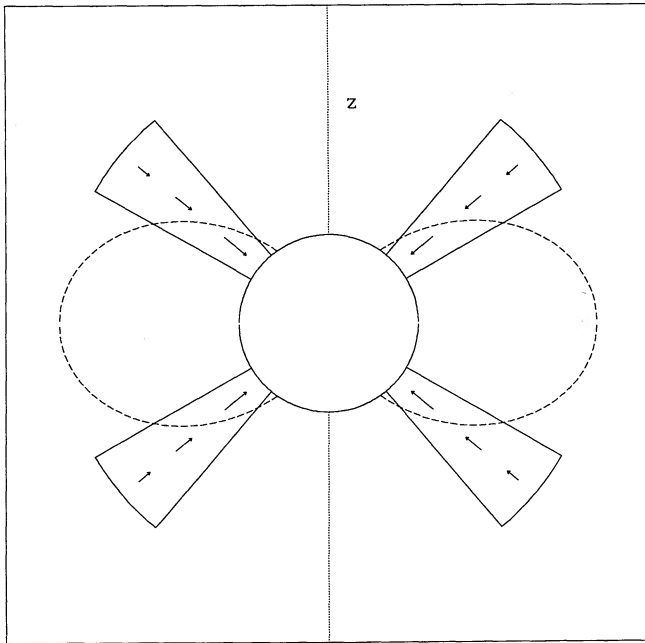


FIG. 1.—Representation of adopted flow geometry in a meridional plane. The figure is azimuthally symmetric around the  $z$ -axis. The infalling material is assumed to flow radially in a cone with latitude limits  $\theta_1, \theta_2$ , measured from the  $z$ -axis. The velocity field corresponds to ballistic infall from the outer edge of the cone,  $3R_*$ . The dashed line represents a dipole field line which has the same maximum radius from the star as the cone.

constant  $r$ , and the envelope temperature is assumed to be isothermal except near the stellar photosphere.

Since most T Tauri stars are slowly rotating, we neglect rotation for an initial exploration. With this approximation, the highly supersonic flow should exhibit nearly ballistic motion (Ghosh, Lamb, & Pethick 1977). Therefore, the adopted velocity field corresponds to ballistic steady radial infall from rest at a specified radius  $r_{\max}$ ,

$$v_p = \left[ \frac{2GM}{R_*} \left( \frac{R_*}{r} - \frac{R_*}{r_{\max}} \right) \right]^{1/2}. \quad (1)$$

For all cases we assume a typical T Tauri stellar mass and radius of  $M_* = 1 M_\odot$  and  $R_* = 3 R_\odot$ , and that the effective temperature of the (undisturbed) photosphere is 4000 K. We further assume that the cone extends to a radial distance  $r_{\max} = 3R_*$ , large enough to produce the substantial velocities of redshifted absorption observed in many YY Orionis stars (e.g., Walker 1972; Edwards 1979; Krautter et al. 1990).

Mass accretion rates of order  $\sim 10^{-7} M_\odot \text{ yr}^{-1}$  are required to explain the excess emission of many T Tauri stars (Bertout et al. 1988; Hartmann & Kenyon 1990). We have calculated infall models using three different density distributions, corresponding to spherically symmetric mass infall rates of  $10^{-7}$  and  $10^{-6} M_\odot \text{ yr}^{-1}$ . Two different latitude ranges are considered,  $20^\circ$  to  $40^\circ$ , and  $40^\circ$  to  $60^\circ$ , for which the total infall rates are 0.174 and 0.266 times the spherically-symmetric values, respectively. Thus, our models span a range of accretion rates from  $1.74 \times 10^{-8}$  to  $2.66 \times 10^{-7} M_\odot \text{ yr}^{-1}$ .

With the adopted stellar mass, radius and  $r_{\max}$ , the velocity of the infalling gas is about  $290 \text{ km s}^{-1}$  immediately above the surface. This material will be decelerated in a strong shock and heated to  $\sim 10^6 \text{ K}$ . The X-ray radiation produced in the shock will be absorbed very close to the shock and reprocessed into ultraviolet and optical radiation which can escape (Königl 1991). The optical and ultraviolet continuum emission produced in this process is likely to be fairly optically thick (see Königl 1991). Assuming that the kinetic energy of the accreted material is converted into blackbody emission from the base of the column, the effective temperature of this region is  $\sim 4000$  and  $7100 \text{ K}$  for spherically symmetric infall rates of  $10^{-7}$  and  $10^{-6} M_\odot \text{ yr}^{-1}$ , respectively. The latter temperature is comparable to observational estimates of the characteristic temperatures of the blue-ultraviolet excess emission of T Tauri stars  $\sim 8000 \text{ K}$  (Bertout et al. 1988; Kenyon & Hartmann 1987). We have adjusted the density and temperature structures of our models close to the stellar surface to achieve Balmer and Paschen continuum emission roughly consistent with these effective temperatures.

Because the X-ray radiation produced by the accretion shock is absorbed in a very short distance, these photons cannot be used to ionize and heat the infalling gas. But the infalling material must be heated to an appreciable temperature in order to produce any Balmer line emission. In the absence of a detailed model for heating the infalling material, we simply assume that it is isothermal at  $7000 \text{ K}$ . This temperature is lower than typically adopted in wind models for the Balmer lines (e.g., Natta, Giovanardi, & Palla 1988; Hartmann et al. 1990), but our accretion cones are much denser than typical wind models. The adoption of much higher temperatures would result in radiative losses from the accretion cones in excess of the accretion luminosity.

The source functions and profiles for the Balmer lines are

calculated using the escape probability methods described in Paper II. We begin by calculating ion and electron densities for the given temperature and total hydrogen density at each radius using the PANDORA radiative transfer code in spherical symmetry (Avrett & Loeser 1984). The PANDORA calculations assume a Sobolev escape probability in the rapidly-expanding regions, and a static escape probability for the slowly moving portions of the atmosphere (see Paper I). The radiative transfer and statistical equilibrium equations for an eight level model hydrogen atom are iterated until convergence. Further details are given in Paper I.

The hydrogen level  $n=1-4$  populations from the spherically-symmetric calculation are used to determine continuum opacities and line escape probabilities. The escape probabilities, which depend on the location ( $r_*$  and  $\theta$ ) inside the cone, are used in the solution of the statistical equilibrium equations for an eight-level hydrogen atom. The  $n=1$  level populations are assumed fixed, with the net radiative brackets for Ly $\alpha$ , H $\alpha$ , H $\beta$ , H $\gamma$ , P $\alpha$ , P $\beta$ , and Br $\alpha$  set equal to the corresponding escape probabilities. The escape probabilities for all Lyman lines have been assumed to be equal to that of Ly $\alpha$ .

A typical solution is shown in Figure 2, where we exhibit the H $\alpha$  line source functions for the  $\theta = 20^\circ-40^\circ$ ,  $\dot{M} = 1.74 \times 10^{-7} M_\odot \text{ yr}^{-1}$  model. As expected, the line source function is largest near the center of the cone and lowest near the edges and end of the cone. The level populations and line source functions do not differ substantially from the spherical solutions over much of the cone, because collisional rates tend to control the results at large optical depths. Only at the edges and end of the cone do the line source functions depart appreciably from the spherical results.

The quantitative details of the profiles are uncertain because they are sensitive to the approximate nature of the solutions at the cone boundaries. The solution of the statistical equilibrium equations results in different populations for  $n \geq 2$  than were used to calculate the Balmer line optical depths and hence the escape probabilities. In principle, the solutions should be iterated to convergence, but this would be very time-consuming because of the absence of spherical symmetry. The computed source functions display the expected qualitative behavior, and

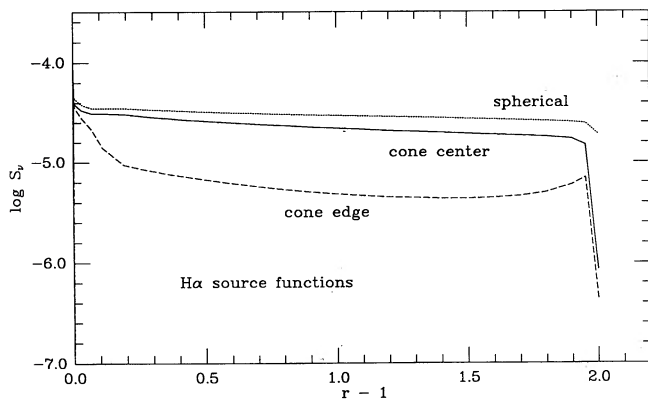


FIG. 2.—The behavior of the H $\alpha$  line source function at the center and edge of a cone, for an infall model with latitude limits  $\theta_1 = 20^\circ$ ,  $\theta_2 = 40^\circ$ , and net mass inflow rate of  $1.74 \times 10^{-7} M_\odot \text{ yr}^{-1}$ . The line source function near the cone center is close to the spherical result; at the edges and end of the cone, the source function decreases because of increased photon escape. The slight rise in the “edge” source function near the end of the cone results from effects described in Paper II.

approach the PANDORA spherically symmetric, self-consistent results in the limit of wide cones. Considering the absence of constraints on the temperature structure of the flow, we feel that our approximate approach is justified for an initial exploration of the problem.

### 3. RESULTS FOR RADIAL FLOW

In Figure 3 we show the calculated Balmer line profiles for the adopted radial infall velocity field and low ( $1.19 \times 10^{-8}$  and  $1.74 \times 10^{-8} M_\odot \text{ yr}^{-1}$ ) accretion rates. The H $\alpha$ , H $\beta$ , and H $\gamma$  profiles are displayed for four different viewing angles  $i$  measured from the  $z$ -axis ( $i = 0^\circ$  corresponds to viewing the system pole-on). The H $\beta$  and H $\gamma$  line profiles exhibit clear inverse P Cygni profiles, with substantial redshifted absorption. The H $\alpha$  profiles are also inverse P Cygni in character, although with much less prominent redshifted absorption. For the case of a nearly polar cone ( $\theta_1 = 20^\circ$ ,  $\theta_2 = 40^\circ$ ; *solid lines*), the redshifted absorption is strongest at low inclination angles ( $10^\circ-30^\circ$ ), where the line of sight is along one side of the cone, and weak or absent when viewed almost equator-on ( $i = 80^\circ$ ), as expected.

For higher accretion rates (Fig. 4), the line profiles of H $\alpha$  show very little evidence for redshifted absorption. The large optical depths of H $\alpha$  in these models results in thermalization of the line source function near the base of the accretion cone. The high temperature of the infalling gas produces line emission which is brighter than the underlying continuum, and so the infalling material produces excess emission, not absorption, on the long-wavelength side of the line profile. The small redshift of the central absorption is produced in the outer regions, where the model geometry is particularly unrealistic (see § 4). Thus, the absence of redshifted absorption in H $\alpha$  does not rule out infall, particularly when redshifted absorption components are seen simultaneously in the higher Balmer series. The high-velocity redshifted absorption is weaker in H $\beta$  and H $\gamma$  in the models with larger accretion rates, and it is clearly possible to construct infall models with no apparent redshifted absorption in the higher Balmer lines at any viewing angles. In addition, redshifted absorption may also not appear for polar infall viewed nearly equator-on (see the  $i = 80^\circ$ ,  $\theta_1 = 20^\circ$ ,  $\theta_2 = 40^\circ$  profiles in Figs. 3 and 4).

Bastian (1982) constructed spherically symmetric infall models for YY Orionis stars in which redshifted absorption was also present in H $\beta$  and H $\gamma$  but not in H $\alpha$ . Bastian adopted higher envelope temperatures than in our accretion columns to achieve this effect, principally because he used higher brightness temperatures for the underlying continuum.

The effect of the far-side accretion column on the line profile is generally to increase the amount of blueshifted emission. This accounts for the “bump” on the blue wing seen, for example, in the  $i = 10^\circ$  line profiles in Figure 4. The structure of this feature is such that it might be mistakenly interpreted, not as excess emission, but as a blueshifted absorption feature from a wind affecting the underlying blue wing emission.

### 4. INFALL WITH DIPOLE VELOCITY FIELD

The only hint of infall in the H $\alpha$  profiles of Figure 4 is given by the slightly redshifted central absorption. This feature is produced in the outermost regions of our model, where our simplified geometry is least likely to be correct. Comparison of adopted geometry of our model with the dipole field line which would intersect the disk at  $3R_*$  (Fig. 1), shows that the cone model does not account for the flow of material near the disk,

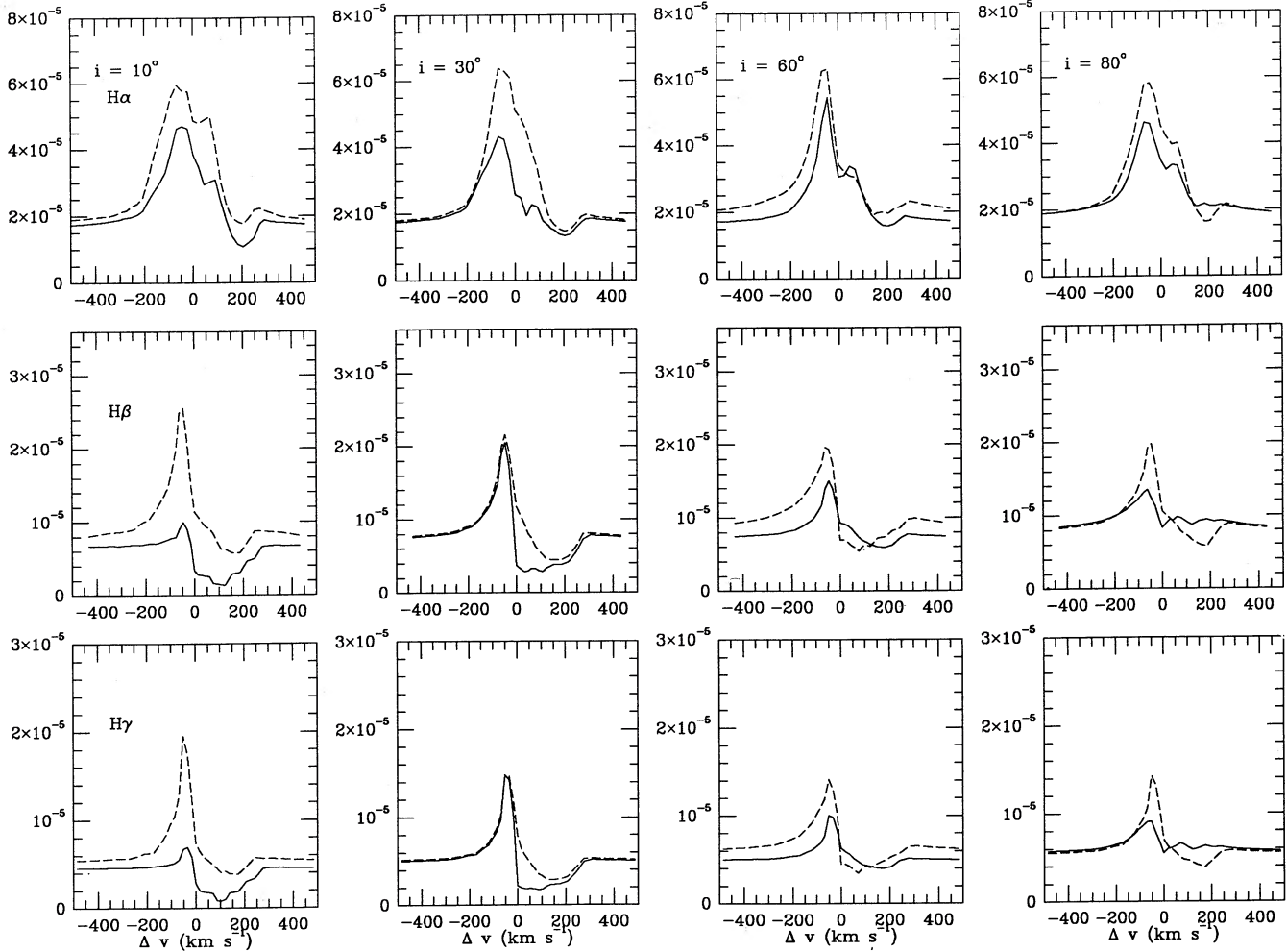


FIG. 3.—Calculated line profiles for H $\alpha$ , H $\beta$ , and H $\gamma$  for 7000 K infall models. The flow is confined to latitude limits  $\theta_1 = 20^\circ$ ,  $\theta_2 = 40^\circ$  (solid line) or to  $\theta_1 = 40^\circ$ ,  $\theta_2 = 60^\circ$  (dotted line), corresponding to total mass accretion rates of  $\dot{M} = 1.74 \times 10^{-8}$  and  $2.66 \times 10^{-8} M_\odot \text{ yr}^{-1}$ , respectively. The profiles are shown for four different viewing angles  $i$  measured from the  $z$ -axis ( $i = 0^\circ$  corresponds to viewing the system pole-on).

which is supposed to be the source of the accreted gas, although the details of this flow are uncertain (see Ghosh & Lamb 1979a, b; Arons et al. 1984; Camenzind 1990; Spruit & Taam 1990).

As can be seen in Figure 1, if the flow were restricted to a magnetic flux tube in dipole geometry, the infall velocity field will not be strictly radial. In order to investigate the qualitative effects that might be produced by true dipole flow, we constructed a crude model of a dipole flow, retaining cone geometry but using the velocity field arising from ballistic infall along an undistorted dipole field line. A dipole streamline is given by

$$r = K \sin^2 \theta \quad (2)$$

(see Ghosh, Lamb, & Pethick 1977), where  $K$  is a constant. The magnetic field components in the  $xz$ -plane are

$$B_x = \frac{3m \sin \theta \cos \theta}{r^3}, \quad (3)$$

$$B_z = \frac{m(3 \cos^2 \theta - 1)}{r^3}, \quad (4)$$

and the total magnetic field is

$$B = \frac{m(4 - 3 \sin^2 \theta)^{1/2}}{r^3}, \quad (5)$$

where  $m$  is the magnetic moment.

Assuming that the field lines are undistorted and the flow is coupled to the field, the velocity is parallel to the field lines. Thus, the velocity in the  $xz$ -plane is

$$\mathbf{v} = -v_p \left[ \frac{3y^{1/2}(1-y)^{1/2}\hat{x} + (2-3y)\hat{z}}{(4-3y)^{1/2}} \right], \quad (6)$$

where  $y = r/K$ ,  $1/K \leq y \leq 1$ . Assuming that the gas pressure is negligible, the Bernoulli constant for our nonrotating model implies that the poloidal velocity  $v_p$  is given by equation (1) (Ghosh, Lamb, & Pethick 1977), with  $r_{\text{max}} = K$ . The position  $r = r_{\text{max}}$  corresponds to  $\theta = \pi/2$  by equation (2), i.e., the disk plane. If the unit vector  $\mathbf{n}$  toward the observer is  $(\sin i \cos \phi \hat{x}, \sin i \sin \phi \hat{y}, \cos i \hat{z})$ , the observed radial velocity is

$$\mathbf{v} \cdot \mathbf{n} = -v_p \left[ \frac{3y^{1/2}(1-y)^{1/2} \sin i \cos \phi + (2-3y) \cos i}{(4-3y)^{1/2}} \right]. \quad (7)$$

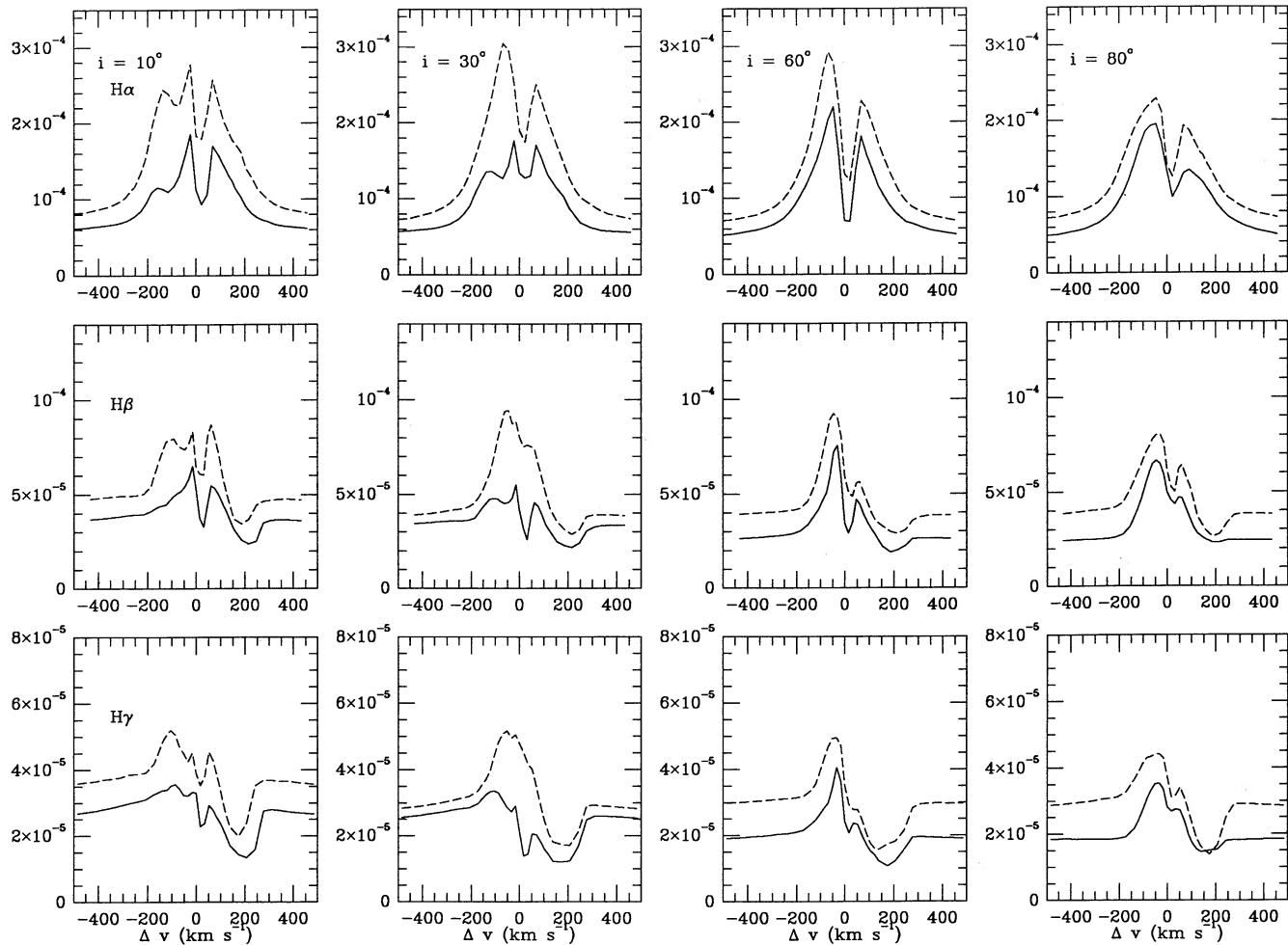


FIG. 4.—Same as Fig. 3, but for mass accretion rates  $\dot{M} = 1.74 \times 10^{-7}$  and  $2.66 \times 10^{-7} M_{\odot} \text{ yr}^{-1}$ . The underlying continuum has a brightness temperature  $\sim 7000 \text{ K}$  (see text).

Equation (7) implies that an observer viewing the system along the polar ( $\hat{z}$ ) axis may observe a blueshift (positive velocity along the  $\hat{z}$ -axis) in the outer part of the field line, where  $2/3 \leq y \leq 1$ . This material is relatively slowly moving, and so can produce a narrow, blueshifted absorption or emission component.

We adopt a cone with latitude limits of  $40^{\circ}$ – $80^{\circ}$ , viewed at  $i = 10^{\circ}$ , and use the velocity field given by equation (3), taking  $K = 3$  to correspond to infall from a disk radius of  $3R_*$ . We further assume for simplicity that the velocity field is constant on surfaces of constant  $r$ . Figure 5 shows results of this modified cone model, adopting the same density and temperature structure used for the models exhibited in Figure 4. This crude model for dipole flow produces line profiles that are very similar to those obtained for radial flow in cone geometry, except that now the central absorption reversal is slightly blueshifted instead of redshifted. This blueshift is produced by the flow of the material up away from the disk plane (see eq. [6]). Note, however, that the velocity field corresponds to monotonically accelerating infall toward the star.

#### 4. DISCUSSION

The broad emission lines of T Tauri stars have generally been assumed to originate in winds (see Paper II, and refer-

ences therein). Outflow models naturally explain the presence of blueshifted absorption in the optically thick lines and blueshifted emission in the optically thin lines (see, e.g., Edwards et al. 1987). However, when examined in detail, wind models have difficulties in explaining the symmetry of many observed line profiles (e.g., DeCampli 1981), the tendency for the emission to be “centrally peaked,” and the occasional appearance of redshifted absorption (Walker 1972; Herbig 1977; Wolf et al. 1977; Appenzeller et al. 1978; Edwards 1979).

These difficulties are summarized in Figure 6, where we display  $H\alpha$  profiles for two T Tauri stars compared with the predicted profiles of wind models from Papers I and II. As discussed in Paper II, simple spherically symmetric, accelerating wind models which tend to produce line profiles that are far too asymmetric in comparison with observations. Wind models with large turbulent velocities and cone geometry produce more symmetric profiles in better agreement with observations, as shown by the top right panel in Figure 6. However, the large turbulent velocities used in these models result in square-looking profiles, whereas many T Tauri show an emission peak near line center (Fig. 6; see also Paper II). Reducing the turbulent velocities does not help because then the line profiles once again become very asymmetric.

In contrast, infall model profiles (Fig. 6) can produce fairly

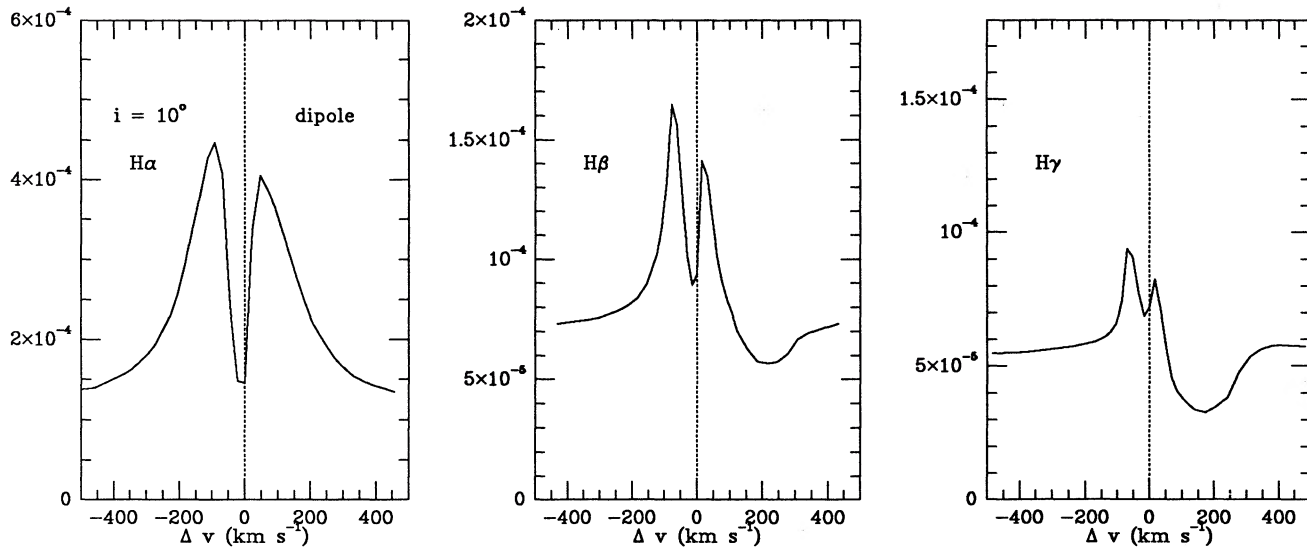


FIG. 5.—Computed line profiles for a cone with  $\theta_1 = 40^\circ$ ,  $\theta_2 = 80^\circ$ , viewed nearly pole-on  $i = 10^\circ$  with the same density and temperature structure as Fig. 4, but adopting a velocity field intended to crudely simulate flow along a dipole magnetic field line. The overall properties of the line profiles are similar to those of Fig. 4, except that the narrow absorption feature is now slightly blueshifted.

symmetric profiles, with emission wings that are qualitatively similar to those observed. It is possible to produce line profiles with central, narrow absorption features, or even centrally peaked emission, as often observed (compare to GG Tau in Fig. 6). These results do not depend upon our approximate solutions for the line source functions, because we find the same qualitative behavior for wide cones, for which our methods are most accurate.

The infall models can explain centrally peaked line profiles that are difficult to reproduce with wind models. To emphasize this point, we have superposed a model infall profile on an H $\alpha$  profile of BP Tau in Figure 7. The general tendency of the peak of the H $\alpha$  line to occur slightly blueward of line center in BP Tau (compare also Basri et al. 1989) is very difficult to achieve in an axisymmetric wind model (Paper II) but is nicely accounted for by infall. Comparison of Figures 3 and 4 shows that the redshifted absorption component in the model could easily be eliminated by slightly increasing the mass infall rate. Significantly, the Na I resonance lines of BP Tau, observed at the same time as H $\alpha$ , exhibit absorption components redshifted by  $\sim 150 \text{ km s}^{-1}$  (Fig. 7; see also the Na I spectrum of BP Tau shown by Hartigan et al. 1989).

Infall models generally have been dismissed because there is often no evidence of redshifted absorption in H $\alpha$  (e.g., Herbig 1977). Our results show that it is quite possible to produce H $\alpha$  line profiles with little or no apparent redshifted absorption in infalling envelopes. The models indicate that the higher Balmer series lines are more likely to exhibit redshifted absorption than H $\alpha$ , consistent with observations (Walker 1972; Herbig 1977; Wolf et al. 1977; Herbig 1977; Appenzeller et al. 1978; Edwards 1979).

Grinin & Mitskevich (1991) show that stochastic wind models with strongly decelerating flow also produce centrally peaked emission line profiles. This is consistent with our results, since the strongly decelerating flow is qualitatively the same velocity field as the infall model, but with opposite sign. The Grinin & Mitskevich (1991) line profiles show absorption reversals with small blueshifts, while our nondipole models show small redshifts. Constructing hydrodynamic wind models

with asymptotic velocities well below the surface escape velocity, as required by the Grinin & Mitskevich (1991) models, is difficult (Holzer, Fla., & Leer 1983).

In Figure 8 we compare the dipole velocity field calculation for H $\beta$  with an observed H $\alpha$  profile of GI Tau. Unlike other T Tauri stars observed at similar signal-to-noise levels, the red wing continuum level in GI Tau is not flat, but is modified by weak redshifted absorption, which is present at the same time that a narrow, slightly blueshifted absorption component is seen. Although the model is very crude, the comparison suggests that the observed GI Tau H $\alpha$  profile may be explained by flow along a dipole field line. Profiles with simultaneous redshifted and blueshifted absorption components have also been observed in the H $\beta$  and H $\gamma$  lines of DF Tau (Hartmann 1982) and in the high Balmer series of S CrA (Wolf et al. 1977). The recent observations of S CrA by Krautter et al. (1990) show this behavior at an epoch when the Na I lines exhibited strong redshifted absorption. While it is possible to explain these observations by separated infalling and expanding regions (Bertout 1979b; Grinin & Mitskevich 1991), it is suggestive that blueshifted and redshifted components can be produced using a simple, physically motivated velocity field.

Our models predict that high-velocity redshifted absorption is most likely to be seen in H $\alpha$  when the emission is relatively weak, because weak emission corresponds to low line optical depths and therefore less thermalization. There is some evidence for this effect; while typical strong-emission T Tauri stars have H $\alpha$  equivalent widths  $\sim 10$ – $100 \text{ \AA}$ , the H $\alpha$  profile of GI Tau in Figure 8 has an emission equivalent width of  $\sim 12 \text{ \AA}$ , and the H $\alpha$  profile of DN Tau in Paper II with redshifted absorption has an equivalent width of approximately  $8 \text{ \AA}$ . (Of course, if the weak H $\alpha$  emission arises entirely from a stellar chromosphere, and no disk accretion is occurring, [e.g., Walter et al. 1988; Strom et al. 1989], then inverse P Cygni profiles are not expected.)

T Tauri stars do have winds, as shown by the observations of forbidden-line emission (Appenzeller et al. 1984; Edwards et al. 1987), and the optically thick lines of some stars show normal P Cygni structure of the type easily explained by wind

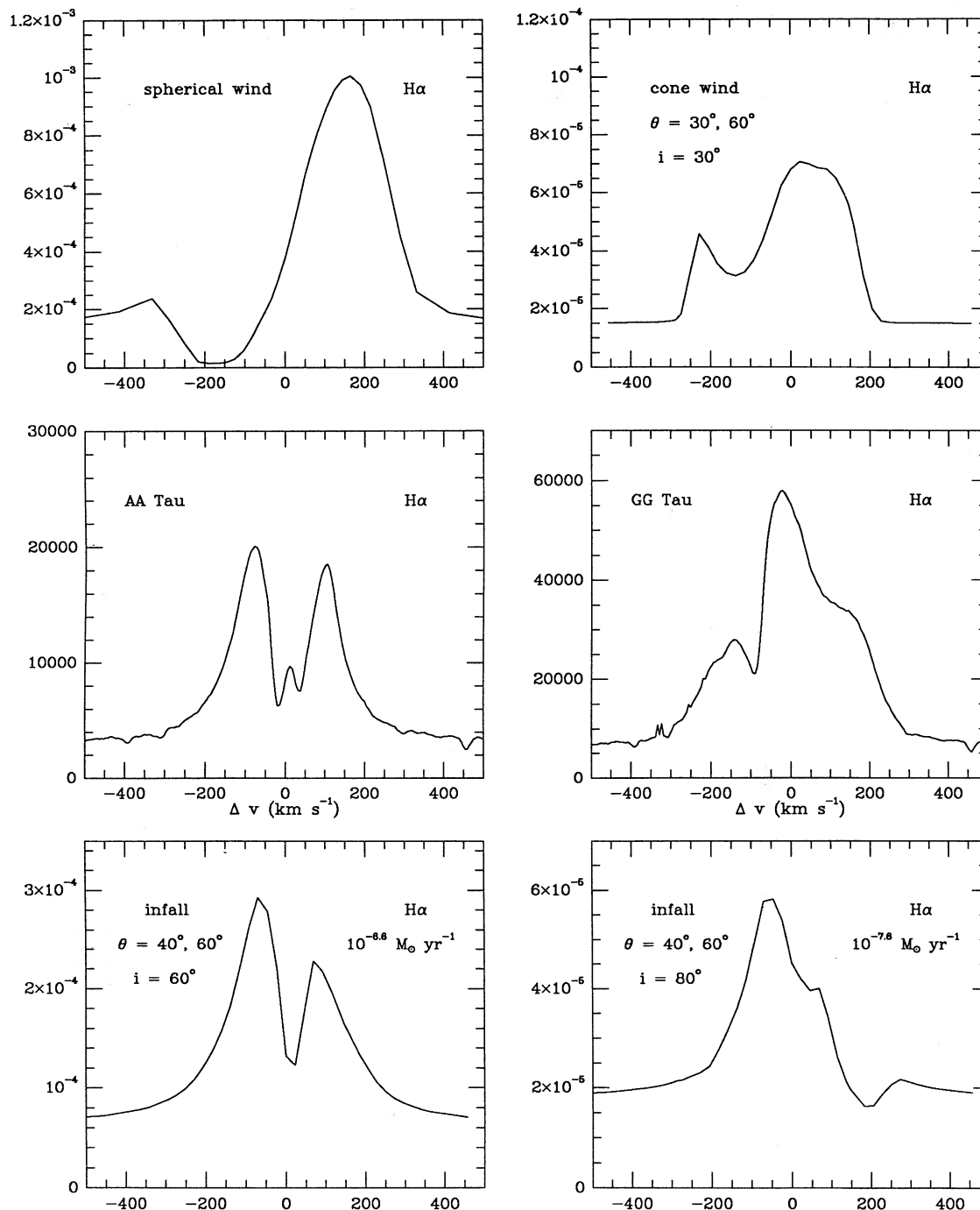


FIG. 6.—H $\alpha$  line profiles for a spherical wind model from Paper I, a “cone” wind model from Paper II, and two infall models, compared with observed profiles of two T Tauri stars. The H $\alpha$  line profiles of AA Tau and GG Tau have resolutions of approximately  $12 \text{ km s}^{-1}$ , and were obtained in 1988 December using the echelle spectrograph and TI-2 CCD detector on the KPNO 4 m telescope. Other details of observations and data reduction are the same as in Hartigan et al. (1989). The bottom left infall profile is from Fig. 4, for the  $\dot{M} = 2.66 \times 10^{-7} M_{\odot} \text{ yr}^{-1}$ ,  $\theta_1 = 40^\circ$ ,  $\theta_2 = 60^\circ$  model viewed at an inclination angle of  $60^\circ$ ; the bottom right infall profile is from Fig. 3, for the  $\dot{M} = 2.66 \times 10^{-8} M_{\odot} \text{ yr}^{-1}$ ,  $\theta_1 = 40^\circ$ ,  $\theta_2 = 60^\circ$  model viewed at an inclination angle of  $80^\circ$ .

models. However, much of the underlying *emission* in the Balmer lines could still come from an accretion flow, while the *absorption* components come from a less dense, overlying wind. Furthermore, it is possible that the sharp absorption components sometimes observed with blueshifts much less than the stellar escape velocity actually arise in dipole infall geometry.

Centrally peaked emission profiles are obtained only if the

turbulent velocity field in the outer envelope is relatively small. Thus, the infall models suggest that previous inferences of “turbulence” in T Tauri winds from the emission profiles of permitted lines (DeCampli 1981; Hartmann, Edwards, & Avrett 1982; Paper I) are incorrect. Furthermore, the use of Brackett and Paschen lines to constrain mass-loss rates (Natta et al. 1988) may be misleading, since these lines could be

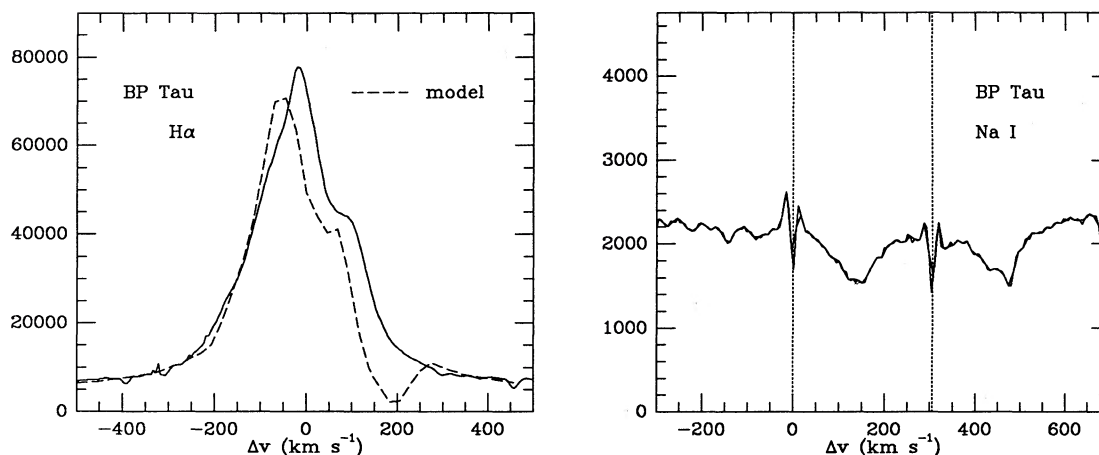


FIG. 7.—The H $\alpha$  and Na I line profiles of BP Tau observed in 1988 December using the KPNO 4 m echelle, as in Fig. 6. The dashed line is an H $\alpha$  profile taken from Fig. 2, for the  $\dot{M} = 2.66 \times 10^{-8} M_{\odot} \text{ yr}^{-1}$ ,  $\theta_1 = 40^\circ$ ,  $\theta_2 = 60^\circ$  model viewed at an inclination angle of  $80^\circ$ .

formed in the same accretion column as the high Balmer series lines. The best tests of the infall hypothesis will be provided by intensive observations of the line profiles of the high Balmer lines and other species formed in the inner emission envelope.

It must be emphasized that the appearance of redshifted absorption depends critically on the temperature of the infalling gas, for which we have no adequate theory. The cooling times of the envelope are short and the gas needs to be continually heated. The large column densities involved make it appear very unlikely that radiation from the accretion shock can penetrate upwards any great distance to ionize and heat the inflow. Scheurwater & Kuijpers (1988) suggest that inhomogeneous accretion into T Tauri stellar magnetospheres could produce sizeable amounts of MHD waves, and perhaps these waves could be used to heat the infalling gas. Without a more definite theory for the temperature structure of the accreting material, it is difficult to make very detailed predictions for the absorption components.

Our present models do not represent the outermost regions of the flow very satisfactorily, because of the cone geometry adopted and because of our neglect of rotation, which should be most significant at the largest radii. Investigations of the

effects of a dipole geometry and rotation on infall line profiles are needed.

## 5. SUMMARY

We have presented line profiles for H $\alpha$ , H $\beta$ , and H $\gamma$ , calculated for ballistic infall in restricted latitude bands onto T Tauri stars, using an escape probability treatment to compute source functions in optically thick, non-spherically symmetric atmospheres. H $\alpha$  line profiles can be surprisingly symmetric, showing little evidence for infall, with a velocity field that produces strong redshifted absorption in the higher Balmer lines. Redshifted absorption is most likely to be seen in H $\alpha$  when the emission is relatively weak, because weak emission corresponds to low line optical depths and therefore less thermalization. T Tauri stars with modest H $\alpha$  line strengths should be monitored for potential inverse P Cygni structure.

We suggest that the Balmer emission lines of many “classical” or “strong-emission” T Tauri stars are produced in an accretion column, with material originating in a circumstellar disk and channeled by the stellar magnetic field, as envisaged by Camenzind (1990) and Königl (1991). The winds of these objects may only produce the observed blueshifted

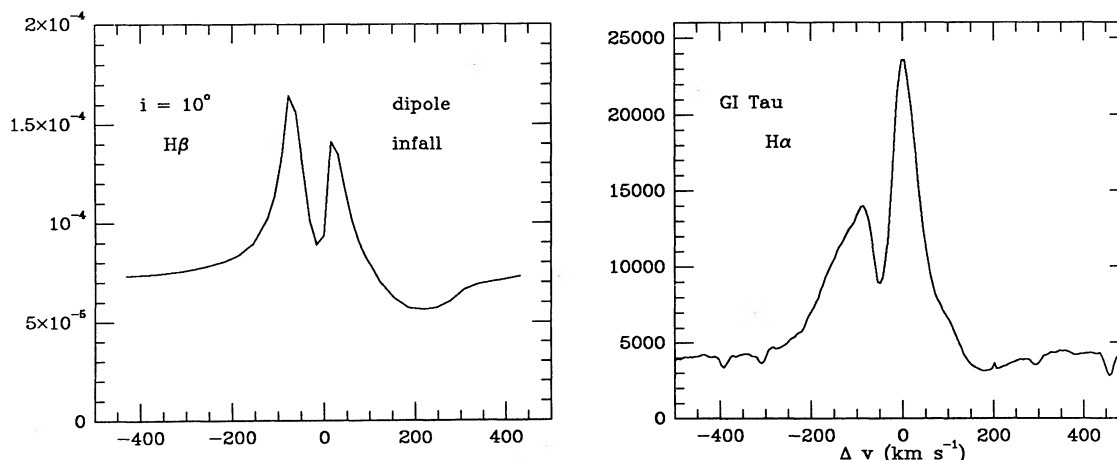


FIG. 8.—Comparison of the dipole model H $\beta$  profile (Fig. 5) with a KPNO 4 m echelle H $\alpha$  spectrum of GI Tau, also obtained in 1988 December, with the same instrumental setup as in Fig. 6. Weak, broad, redshifted absorption in GI Tau is present at the same time that a narrow blueshifted absorption component is also seen, qualitatively similar to the dipole model profile.

absorption without substantial emission. Some of the sharp, slightly blueshifted absorption components seen in the Balmer lines could arise from a purely *infalling* envelope in dipole geometry.

We acknowledge useful conversations with Arieh Königl and Max Camenzind. Suzan Edwards contributed very helpful

comments on a previous version of this manuscript, and made her echelle observations of high Balmer series line in T Tauri stars available to us. We also thank Gibor Basri for helpful discussions and for kindly providing observed line profiles of T Tauri stars for our inspection. This work was supported in part by the International Exchange Program of the Smithsonian Institution and by NASA grant NAGW-511.

## REFERENCES

- Adams, F. C., Lada, C. J., & Shu, F. H. 1987, *ApJ*, 312, 788  
 Appenzeller, I., Jankovics, I., & Ostreicher, R. 1984, *A&A*, 141, 108  
 Appenzeller, I., Mundt, R., & Wolf, B. 1978, *A&A*, 63, 289  
 Appenzeller, I., & Wolf, B. 1977, *A&A*, 54, 713  
 Arons, J., Burnard, D. J., Klein, R. I., McKee, C. F., Pudritz, R. E., & Lea, S. M. 1984, in *AIP Conf. Proc.*, No. 115, *High Energy Transients in Astrophysics*, ed. S. E. Woosley (New York: AIP), 215  
 Avrett, E. H., & Loeser, R. 1984, in *Methods in Radiative Transfer*, ed. W. Kalkofen (Cambridge: Cambridge Univ. Press), 341  
 Basri, G., & Bertout, C. 1989, *ApJ*, 341, 340  
 Basri, G. B., Rumph, T. F., Batalha, C. C., & Stout, N. M. 1989, *BAAS*, 21, 716  
 Bastian, U. 1982, *A&A*, 109, 245  
 Bertout, C. 1977, *A&A*, 58, 153  
 ———. 1978a, *A&A*, 80, 138  
 ———. 1978b, *Mitt. Astron. Ges.*, 43, 176  
 ———. 1987, in *IAU Symp.* 122, *Circumstellar Matter*, ed. I. Appenzeller & C. Jordan (Dordrecht: Reidel), 23  
 Bertout, C., Basri, G., & Bouvier, J. 1988, *ApJ*, 330, 350  
 Bertout, C., Krautter, J., Möllenhoff, C., & Wolf, B. 1977, *A&A*, 61, 737  
 Bouvier, J., Bertout, C., Benz, W., & Mayor, M. 1986, *A&A*, 165, 110  
 Calvet, N., Hartmann, L., & Hewett, R. 1991, *ApJ*, 386, 229 (Paper II)  
 Camenzind, M. 1990, *Reviews in Modern Astronomy* (Berlin: Springer), in press  
 DeCampli, W. M. 1981, *ApJ*, 244, 124  
 Edwards, S. 1979, *PASP*, 91, 329  
 Edwards, S., Cabrit, S., Strom, S. E., Heyer, I., & Strom, K. M. 1987, *ApJ*, 321, 473  
 Ghosh, P., & Lamb, F. K. 1979a, *ApJ*, 232, 359  
 ———. 1979b, *ApJ*, 234, 296  
 Ghosh, P., Lamb, F. K., & Pethick, C. J. 1977, *ApJ*, 217, 578  
 Grinan, V. P., Mitskevich, A. S. 1991, preprint  
 Hartigan, P., Hartmann, L., Kenyon, S., Hewett, R., & Stauffer, J. 1989, *ApJS*, 70, 899  
 Hartmann, L. 1982, *ApJS*, 48, 109  
 Hartmann, L., Calvet, N., Avrett, E. H., & Loeser, R. 1990, *ApJ*, 349, 168  
 Hartmann, L., Edwards, S., & Avrett, E. H. 1982, *ApJ*, 259, 180  
 Hartmann, L., Hewett, R., Stahler, S., & Mathieu, R. D. 1986, *ApJ*, 309, 275  
 Hartmann, L., & Kenyon, S. J. 1990, *ApJ*, 349, 190  
 Herbig, G. H. 1977, *ApJ*, 214, 747  
 Holzer, T. E., Fla, T., & Leer, E. 1983, *ApJ*, 275, 808  
 Kenyon, S. J., & Hartmann, L. 1987, *ApJ*, 323, 714  
 Königl, A. 1991, *ApJ*, 370, L39  
 Krautter, J., Appenzeller, I., & Jankovics, I. 1990, *A&A*, in press  
 Kuhl, L. V. 1964, *ApJ*, 140, 1409  
 Lamzin, S. 1989, *AZh*, 66, 1329  
 Lynden-Bell, D., & Pringle, J. E. 1974, *MNRAS*, 168, 603  
 Mundt, R. 1979, *A&A*, 74, 21  
 Natta, A., Giovanardi, C., & Palla, F. 1988, *ApJ*, 332, 921  
 Rucinski, S. 1985, *AJ*, 90, 2321  
 Scheurwater, R., & Kuijpers, J. 1988, *A&A*, 190, 178  
 Shu, F. H., Adams, F. C., & Lizano, S. 1987, *ARA&A*, 25, 23  
 Spruit, H. C., & Taam, R. E. 1990, *A&A*, 229, 475  
 Strom, K. U., Strom, S. E., Edwards, S., Cabrit, S., & Skrutskie, M. F. 1989, *AJ*, 97, 1451  
 Ulrich, R. K. 1976, *ApJ*, 210, 377  
 Ulrich, R. K., & Knapp, G. R. 1979, *ApJ*, 230, L99  
 Vogel, S. N., & Kuhl, L. V. 1981, *ApJ*, 245, 960  
 Wagenblast, R., Bertout, C., & Bastian, U. 1982, *A&A*, 120, 6  
 Walker, M. F. 1972, *ApJ*, 175, 89  
 Walter, F. M., Brown, A., Mathieu, R. D., Myers, P. C., & Vrba, F. V. 1988, *AJ*, 96, 297  
 Wolf, B., Appenzeller, I., & Bertout, C. 1977, *A&A*, 58, 163